Facile Route to Organoboron Quinolate Polymers through Boron-Induced Ether Cleavage

Haiyan Li and Frieder Jäkle*

Department of Chemistry, Rutgers University-Newark, 73 Warren Street, Newark, New Jersey 07102

Received January 20, 2009; Revised Manuscript Received March 17, 2009

ABSTRACT: Two new organoboron quinolate polymers were prepared under exceptionally mild conditions via a novel polycondensation reaction involving boron-induced ether cleavage. The polymers, which contain both the boron and quinolato moieties in the main chain, were characterized by multinuclear and 2D NMR, gel permeation chromatography, and matrix-assisted laser desorption ionization time-of-flight (MALDI-TOF) mass spectrometry. They are readily soluble in common organic solvents and thermally stable to >300 °C according to thermogravimetric analysis. The photophysical properties strongly depend on the nature of the conjugated bridge connecting the organoboron quinolato groups. Therefore, with a highly delocalized Th−C_6H_4−Th (Th = thiophene) linker, the lowest energy absorption corresponds to intramolecular charge transfer (ICT) from this conjugated linker to the pyridyl moiety. In contrast, with a less delocalized biphenyl linker, ICT occurs from the fluorene moiety of the diboron monomer to the pyridyl rings on the basis of time-dependent density functional theory (TD-DFT) calculations on molecular model systems. The polymer with the biphenyl linker displays a strong yellow-green emission, whereas the Th−C_6H_4−Th linker shows an unusual concentration-dependent dual emission as a result of excimer formation.

Introduction

Since the first efficient organic light-emitting diode (OLED) based on Alq_3 was reported by Tang and VanSlyke,[1] many studies have focused on other metal or metalloid complexes with 8-hydroxyl quinoline (HQ) and related ligands.[2] Among them, molecular organoboron quinolates and related chelate complexes turned out to be promising because of their good thermal stability and efficient luminescence.[3−7] An important factor for OLEDs being widely commercialized is the processability during fabrication. In this respect, polymeric LEDs (PLEDs) can be advantageous over OLEDs based on molecular materials in that they can often be more easily applied in solution processing using, for example, ink jet printing techniques, thereby allowing for fast and cost-effective manufacture.[8]

Several different approaches have been taken to realize PLEDs based on quinolato complexes. The first one is to attach quinolato moieties to a soluble polymer backbone, followed by metal complexation through post modification.[9] The second method is to prepare a polymer with pendant metal or metaloid moieties first, which is then reacted with quinolato ligands.[7,10] By using such a reverse modification procedure, one can easily prepare a versatile polymer scaffold and subsequently tune the photophysical properties through variations in the substitution pattern of the ligands. Finally, organoboron quinolates and related fluorophores can also be incorporated into the polymer main chain by polycondensation reactions.[11,12] Chujo and coworkers have used this methodology to prepare the first main-chain-type organoboron quinolates with boron embedded in the polymer backbone. They also reported on organoboron quinolate polymers in which the quinolato group is part of the polymer backbone with the organoborane moieties as pendant groups.[12]

Here we report a new type of polymer architecture with both the quinolato ligands and boron centers embedded in the main chain, which was achieved by a simple one-step procedure that involves metal-free boron-induced ether cleavage reactions. This work was inspired by the recent studies by Suning Wang and coworkers on molecular multichromophore assemblies such as **A1** and **A2**, which are derived from polytopic ligands for coordination to multiple metal centers.[5] The complexes **A1** and **A2** were more thermally stable than the related monoboron system.[3,4] Most interestingly, unusual photophysical properties were reported for **A1**. The latter exhibited concentration-dependent dual emission in solution, which was attributed to enhanced excimer formation with increasing concentration. Another objective of our studies was therefore to examine whether the incorporation of these chromophores into polymeric structures would result in interesting luminescence characteristics because of excimer formation.

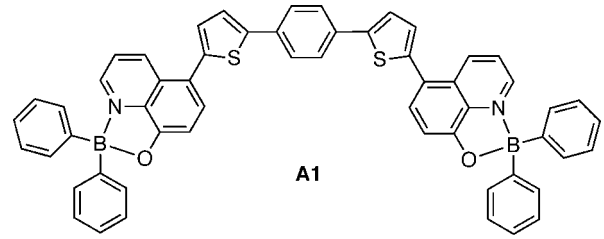

A1

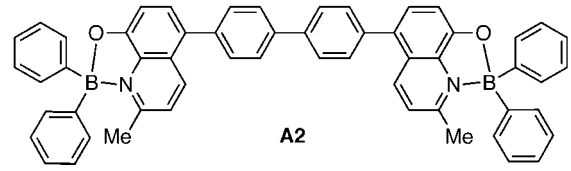

A2

Results and Discussion

The bifunctional organoborane monomer 2,7-bis((*t*-butylphenyl)bromoboryl)-9,9-dihexylfluorene (**B1**) was prepared starting from 2,7-bis(trimethylsilyl)-9,9-dihexylfluorene according to Scheme 1. Boron−silicon exchange was achieved by treatment of 2,7-bis(trimethylsilyl)-9,9-dihexylfluorene with a slight excess of BBr_3 in CH_2Cl_2.[13] Subsequent reaction with 2 equiv of 1-trimethylstannyl-4-*t*-butylbenzene led to selective replacement of one Br substituent on each boron atom, as confirmed by ^1H NMR analysis. The monomer **B1** was purified by repeated recrystallization from hexanes at −35 °C.

* To whom correspondence should be addressed. E-mail: fjaekle@rutgers.edu.

10.1021/ma9001319 CCC: $40.75 © 2009 American Chemical Society
Published on Web 04/13/2009

Scheme 1. Synthesis of Quinolato Polymers

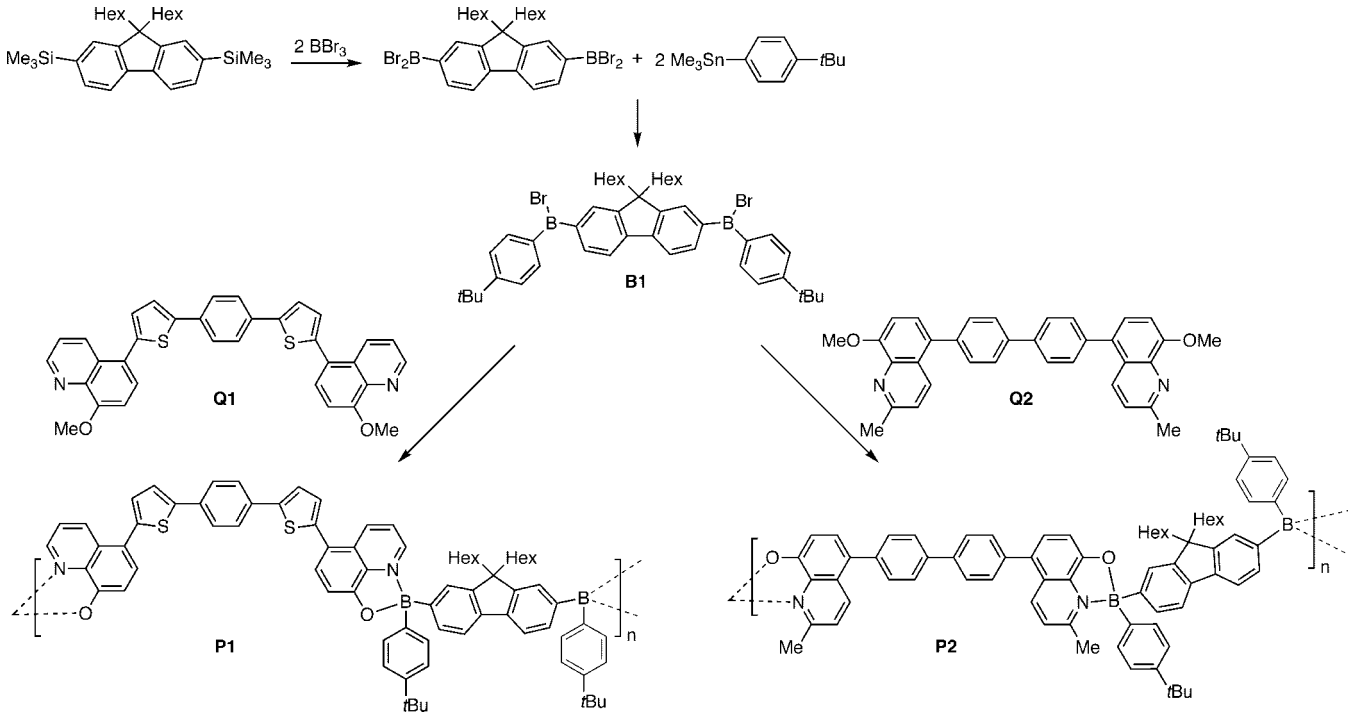

We prepared the organoboron quinolate polymers **P1** and **P2** under mild conditions by simply mixing the bifunctional boron monomer **B1** at RT with the methoxy-protected bifunctional quinolato monomers **Q1** and **Q2**, respectively, followed by stirring for 24 h (Scheme 1). The volatile byproduct MeBr was easily removed under high vacuum. We purified the polymers by adding hexanes to a solution of the crude material in CH_2Cl_2, which led to precipitation of the products. **P1** was isolated as an orange solid in 59% yield and **P2** was isolated as a yellow solid in 66% yield.

Both polymers are readily soluble in typical organic solvents such as CH_2Cl_2, tetrahydrofuran (THF), toluene, and so on. They are stable both as solids and in solution for extended periods of time. The polymers also show good thermal stability on the basis of thermogravimetric analysis (TGA). The onset of the thermal degradation of **P1** was determined to be 326 °C and that of **P2** was determined to be 318 °C.

The chemical structure of the polymers was confirmed by 1D multinuclear NMR spectroscopy and 2D ^{1}H NMR. ^{11}B NMR resonances at 11 ppm for **P1** and at 12 ppm for **P2**, respectively, which are in the typical region of tetracoordinate boron compounds, confirm the attachment of the quinolato groups to boron. For both **P1** and **P2**, the protons of the fluorene and *tert*-butylphenyl moieties experience a strong upfield shift upon chelation by the electron-donating quinolato ligands (Figure 1). Most of the signals for the quinolato moieties and the aromatic bridging groups do not significantly change upon boron coordination. A notable exception is the pronounced downfield shift of one of the quinolato protons in **P2** from 8.24 to 8.55 ppm, which is similar to the chemical shift observed for the respective diboron species **A2** (8.61 ppm)[5] and likely a result of ring current effects (Figure 1). Importantly, all of the major signals can be readily assigned to the expected polymer structures on the basis of 2D NMR experiments (Supporting Information), which is indicative of clean transformations through boron-induced ether cleavage reactions. The absence of additional signals also suggests that the concentration of end groups is small, and hence the polymers are either cyclic or of fairly high molecular weight.

Gel permeation chromatography with in-line multi-angle laser light-scattering detection (GPC-MALLS) in THF gave weight-average molecular weights of $M_w = 1.72 \times 10^4$ (PDI $= M_w/M_n = 1.20$) for reprecipitated samples of **P1** and $M_w = 1.66 \times 10^4$ (PDI $= 1.24$) for **P2**. These results indicate that for each polymer, an average of ca. 25 quinolato moieties are embedded in the polymer chains. We further examined the polymers by high-resolution matrix-assisted laser desorption ionization time-of-flight (MALDI-TOF) mass spectrometry. For both polymers **P1** and **P2**, we were able to detect two different series of peaks, both of which show the expected repeating unit and a chain length of up to $n = 6$. A more detailed analysis suggested that the two different series correspond to fragments with a quinolatoborane moiety at one chain end and a fluorene moiety at the other chain end. The difference between the first and the second series is that the former corresponds to protonated species $[\{RU\}_nH]^+$ (RU = repeating unit), whereas the loss of a *tert*-butylphenyl group is observed for the latter $[\{RU\}_n - t\text{-BuPh}]^+$. (See the Supporting Information.)

The photophysical properties were studied by UV−visible spectroscopy and fluorescence measurements, and the data were supported by density functional theory (DFT) calculations on molecular model systems. The UV−vis absorption spectra of the two polymers in CH_2Cl_2 ($c \approx 10^{-5}$ to 10^{-6} M) are shown in Figure 2. Solutions of **P1** in CH_2Cl_2 are orange, and those of **P2** are yellow. The lowest energy absorption bands are almost identical to those of the respective bifunctional species **A1** and **A2** reported by Wang's group[5] and are therefore likely due to quinolato ligand-based transitions. For instance, **P2** shows a maximum at 411 nm that is red-shifted by only ca. 5 nm relative to that of **A2**. Polymer **P1** shows a band (shoulder) at ca. 443 nm (430 nm for **A1**) and a higher energy maximum at 367 (366 nm for **A1**). The latter band was tentatively attributed to an electronic transition that involves the bridging moiety. The red-shift of this band for **P1** relative to **P2** (ca. 311 nm) is consistent with the higher degree of conjugation of the Th−C_6H_4−Th linker in comparison with the biphenyl group.[5] The observation that the polymer absorptions are similar to those reported for the bifunctional species further confirms the structural integrity

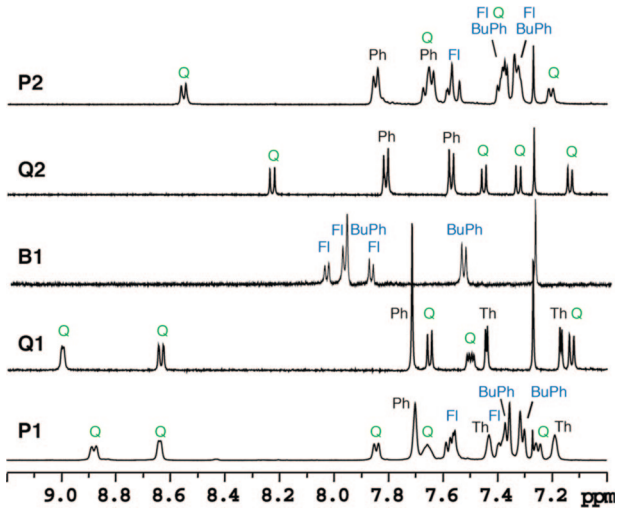

Figure 1. Aromatic region of the ^{1}H NMR spectra of **P1** and **P2** in comparison with **B1** and the ligands **Q1** and **Q2**. (See Scheme 1 for the chemical structures.) Q: quinolato, BuPh: 4-*t*-butylphenyl, Fl: fluorene, Th: thiophene.

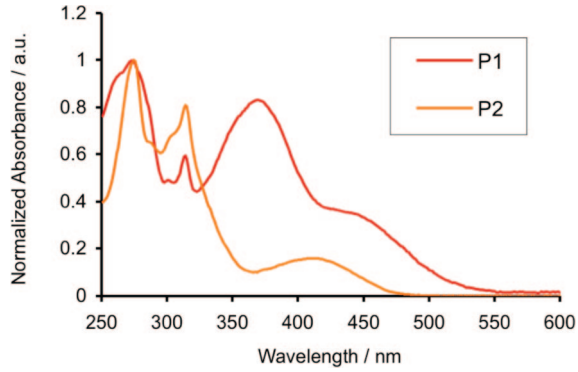

Figure 2. UV−visible spectra of **P1** and **P2** in CH_2Cl_2. (See Scheme 1 for the chemical structures.)

of the polymers with organoboron quinolato chromophores bridging the organic aromatic linkers. At the same time, it strongly suggests that extended electronic communication throughout the polymer chain is very limited because of tetracoordination of the boron moieties.[14]

To confirm the assignments of the absorptions bands for **P1** and **P2** further, we performed DFT calculations on the molecular model systems **M1** and **M2** (Figure 3). Coordination of the quinolato groups leads to the generation of a stereogenic center at boron, and only the structures of the R,R-isomers of **M1** and **M2** were optimized. As reported for other organoboron quinolate complexes, the lowest unoccupied molecular orbital (LUMO) is primarily localized on the pyridyl moiety of the quinolato groups. However, the highest occupied molecular orbital (HOMO) for **M1** and **M2** is different in that for **M1**, the electron density is delocalized on the aromatic Th−C_6H_4−Th linker with contributions from the phenolate part of the quinolate moiety, whereas for **M2**, it is found on the pendant fluorene moieties. The reverse situation is observed for the HOMO-2, which is localized on the fluorene moieties for **M1** and the biphenyl linker/phenolate π system for **M2**. This implies that the HOMO and HOMO-2 exchange positions when going from **M1** with its highly delocalized bridging π system to **M2** with its twisted biphenyl linker.

Time-dependent DFT calculations demonstrate that the lowest energy absorptions indeed correspond primarily to a HOMO-to-LUMO (and for **M2** also HOMO-2) transition. This transition is therefore characterized by charge transfer from the conjugated quinolate linker (for **M1**) and the fluorene moieties (for **M2**) to the pyridyl ring of the quinolato moiety. This is different from the parent compound Ph_2BQ and related organoboron quinolate species, for which the HOMO−LUMO transition typically corresponds to a quinolate-centered charge transfer from the phenolate to the pyridyl moiety. However, it is consistent with studies on organoboron quinolate complexes where organic π systems with extended delocalization are attached in the 5-position of the quinolate ligand.[4,7] For instance, attachment of a benzothiophene group leads to a strong orbital contribution from the benzothiophene moiety to the HOMO level, whereas the LUMO remains centered on the quinolato ligand.[4] Finally, for both **M1** and **M2,** the higher energy band can be assigned to excitation into the LUMO+2, a π^* orbital centered on the bridging aromatic linker.

As noted in the introduction, the unusual emission properties of the bifunctional species **A1** in part prompted us to investigate the respective polymeric materials. The photoluminescence spectra of **P1** and **P2** in CH_2Cl_2 solution (ca. 1×10^{-6} to 1×10^{-7} M) are presented in Figure 4. Independent of the excitation wavelength and concentration, **P2** emits yellow light at a wavelength of $\lambda_{em} = 536$ nm. The emission of **P2** is reminiscent of that of a 5-naphthyl-substituted Ph_2BQ derivative, which was reported to emit at 534 nm with a quantum efficiency of 11%.[4] It is also noteworthy that the emission is only slightly red-shifted compared with the molecular species **A2** ($\lambda_{em} = 528$ nm)[5] and the quantum efficiency of 19% is also similar to that of **A2** (23%).

The emission of **P1** is excitation-wavelength-dependent. When excited at 443 nm, a single emission band was observed at $\lambda_{em} = 611$ nm. This band correlates reasonably well with that found by Wang[5] for **A1** at concentrations >5×10^{-5} M ($\lambda_{em} = 593$ nm), and the relatively low quantum efficiency of ca. 1% is also similar to that of the molecular species. Wang reported that at very low concentrations of **A1**, the emission was centered at $\lambda_{em} = 462$ nm.[5] We found that excitation into the higher energy band of **P1** at 367 nm led to dual emission at $\lambda_{em} = 470$ and 611 nm. Moreover, the lower energy band became relatively more intense with increasing concentration (Figure 4b). This suggests that excimer formation, as postulated for the molecular species,[5] also occurs for the polymeric material at high concentrations.[15] Therefore, despite the incorporation of the organoboron quinolate moieties into the polymeric structure, alignment of the chromophores is still possible, and an interesting concentration-dependent emission behavior due to excimer formation was realized.

Experimental Section

Materials and General Methods. Compounds **Q1**,[5] **Q2**,[5] 1-trimethylstannyl-4-*tert*-butylbenzene,[16] and 2,7-bis(dibromoboryl)-9,9-dihexylfluorene[13] were prepared according to literature procedures. Reactions and manipulations involving reactive boron species were carried out under an atmosphere of prepurified nitrogen using either Schlenk techniques or an inert-atmosphere glovebox (Innovative Technologies). Ether solvents were distilled from Na/benzophenone prior to use. Hydrocarbon and chlorinated solvents were purified using a solvent purification system (Innovative Technologies; alumina/copper columns for hydrocarbon solvents); the chlorinated solvents were distilled from CaH_2 and degassed via several freeze−pump−thaw cycles.

The 499.9 MHz ^{1}H NMR spectra and 125.7 MHz ^{13}C NMR spectra were recorded on a Varian INOVA 500 MHz spectrometer. The 160.4 MHz ^{11}B NMR spectra were recorded with a boron-free probe using boron-free quartz NMR tubes. The ^{1}H and ^{13}C NMR spectra were referenced internally to the solvent peaks, and the ^{11}B NMR spectra were referenced externally to $BF_3 \cdot Et_2O$ ($\delta = 0$) in C_6D_6. The abbreviations *t*-BuPh (4-*t*-butylphenyl), Fl (2,7-fluo-

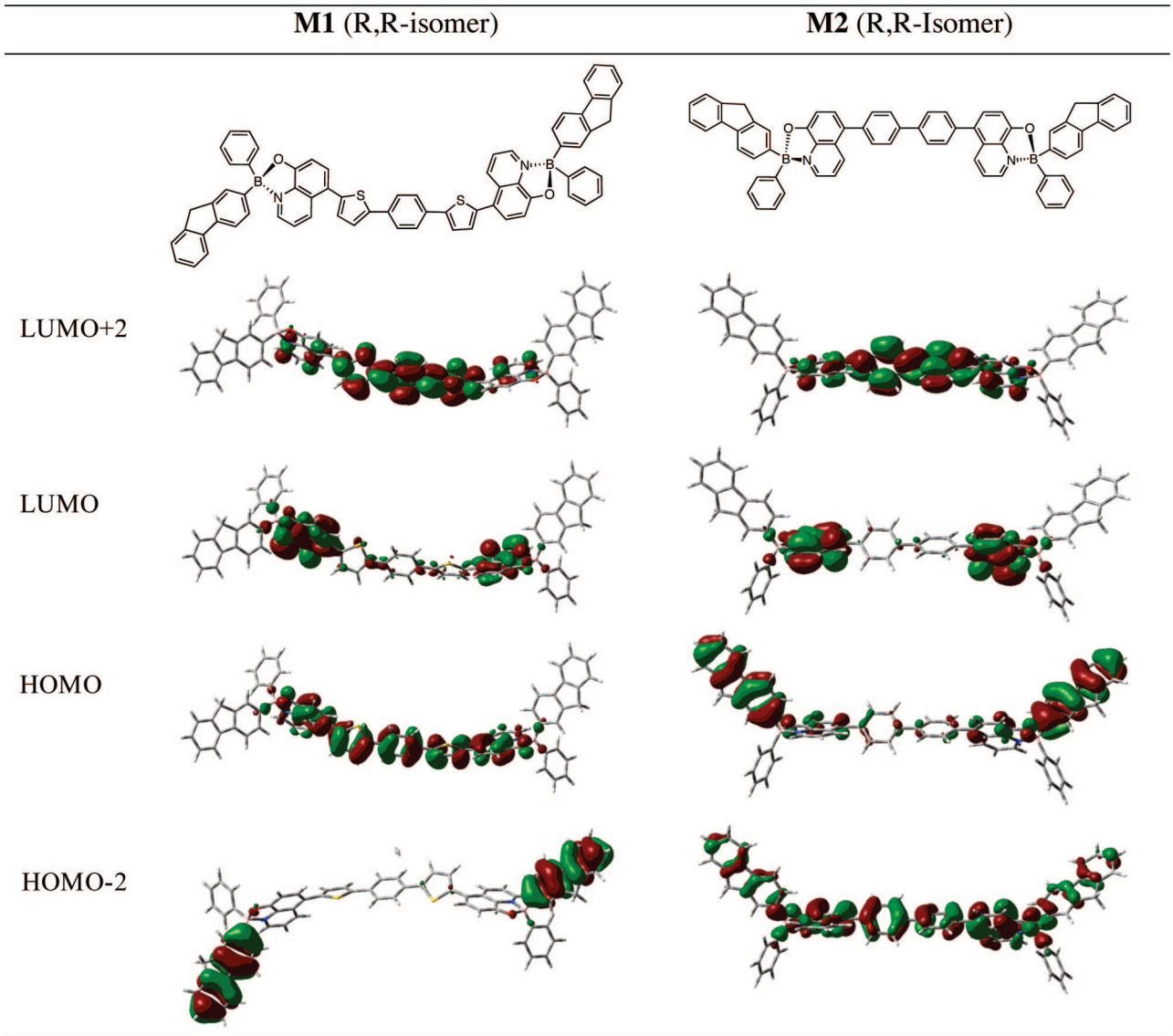

Figure 3. Selected computed (Gaussian03) orbital plots for **M1** and **M2**.

renediyl), and Q (8-hydroxyquinolato) were used for peak assignments. Elemental analyses were performed by Quantitative Technologies (Whitehouse, NJ).

UV−visible absorption data were acquired on a Varian Cary 500 UV−vis/NIR spectrophotometer. The fluorescence data and quantum yields were measured on a Varian Cary Eclipse fluorescence spectrophotometer. Anthracene and diphenylanthracene were used as the standards for determination of the quantum yields as specified. The quantum yields of anthracene (0.33) and diphenylanthracene (0.92) were adopted from the *Handbook of Photochemistry*.[17] Sample solutions were prepared using a microbalance (±0.1 mg) and volumetric glassware.

GPC analyses were performed in THF (1 mL/min) using a Waters Breeze system equipped with a 717plus autosampler, a 1525 binary HPLC pump, a 2487 dual λ absorbance detector, and a 2414 refractive index detector (880 nm). Two styragel columns (Polymer Laboratories; PLgel 5 μm mixed-C, linear range 200−2 000 000), which were kept in a column heater at 35 °C, were used for separation. The columns were calibrated with polystyrene standards (Polymer Laboratories). MALLS experiments were performed at 690 nm (30 mW linear polarized GaAs laser) using a Wyatt Dawn EOS instrument in-line with the GPC; differential refractive indices (d*n*/d*c*) were calculated from in-line GPC-MALLS mode with Wyatt Astra software assuming 100% mass recovery; a Wyatt Optilab refractive index detector operating at 690 nm was used for this purpose. MALDI-TOF measurements were performed on an Applied Biosystems 4700 proteomics analyzer in reflectron (+)-mode with delayed extraction. Benzo[*a*]pyrene was used as the matrix (20 mg/mL toluene). The samples were dissolved in toluene (10 mg/mL), mixed with the matrix in a 1:10 ratio, and then spotted on the wells of a sample plate inside a glovebox. Peptides were used for calibration (Des-Arg-Bradykinin (904.4681), Angiotensin I (1296.6853), Glu-Fibrinopeptide B (1570.6774), ACTH (clip 1-17) (2093.0867), ACTH (clip 18-39) (2465.1989), ACTH (clip 7-38) (3657.9294)) with α-hydroxy-4-cyanocinnamic acid as the matrix. TGA measurements were performed on a Perkin-Elmer Pyris 1 thermogravimetric analyzer under a N_2 atmosphere at a scan rate of 20 °C/min and up to 800 °C.

DFT calculations were performed with the Gaussian03 program.[18] Geometries and electronic properties are calculated by means of hybrid density functional B3LYP with the basis set of 6-31G(d). The input files and orbital representations were generated with Gaussview (scaling radii of 75%, isovalue of 0.02). Excitation data were calculated using TD-DFT (B3LYP).

Synthesis of 2,7-Bis(4-*t*-butylphenylbromoboryl)-9,9-dihexylfluorene (B1). At −35 °C, a solution of 1-trimethylstannyl-4-*tert*-butylbenzene (230 mg, 0.74 mmol) in 10 mL of CH_2Cl_2 was added to a solution of 2,7-bis(dibromoboryl)-9,9-dihexylfluorene (251 mg, 0.37 mmol) in 5 mL of CH_2Cl_2. The mixture was allowed to warm up to room temperature and was stirred for 4 h. The volatile

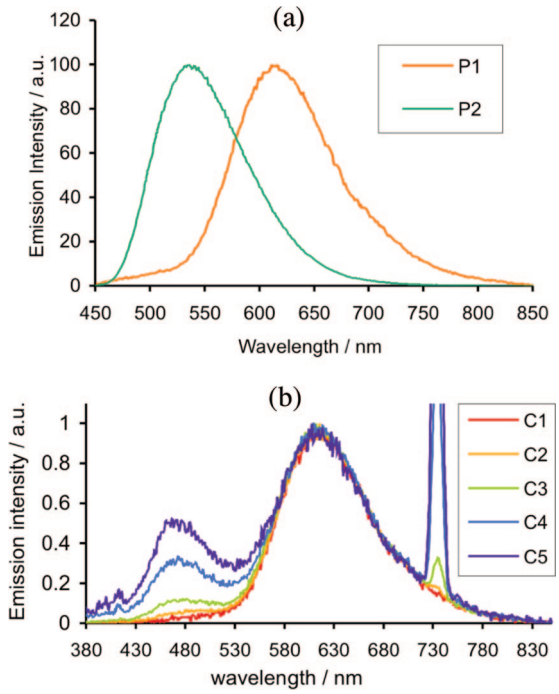

Figure 4. (a) Emission spectra of **P1** (1.04×10^{-6} M repeat units, excited at 443 nm) and **P2** (4.0×10^{-7} M repeat units, excited at 411 nm). (b) Concentration dependence of the emission of **P1**; concentration of repeat units: C1 = 2.73×10^{-5} M, C2 = 1.36×10^{-5} M, C3 = 6.80×10^{-6} M, C4 = 1.70×10^{-6} M, C5 = 8.5×10^{-7} M; $\lambda_{exc} = 367$ nm. (The signal at 734 nm is due to the half-harmonic of the excitation pulse.)

materials were removed under high vacuum, and the residue was purified by crystallization from hexanes at −35 °C. Yield: 210 mg, 72%. ^{1}H NMR ($CDCl_3$, δ): 8.07 (d, 2H, ^3J = 7.5 Hz, Fl), 8.00 (m, 6H, ^3J = 8.6 Hz, Ph and Fl), 7.90 (d, 2H, ^3J = 8.0 Hz, Fl), 7.55 (d, 4H, ^3J = 8.0 Hz, Ph), 2.07 (m, 4H, Hex-CH_2), 1.41 (s, 18H, *t*-Bu), 1.06−1.20 (br, 12H, Hex-CH_2), 0.81 (t, 6H, ^3J = 7.0 Hz, Hex-CH_3), 0.74 (br, 4H, Hex-CH_2). ^{13}C NMR ($CDCl_3$, δ): 157.1 (Ph), 151.3 (Fl), 145.0 (Fl), 140.1 (Fl), 138.1 (Ph), 137.4 (Ph), 137.1 (Fl), 132.2 (Fl), 125.2 (Ph), 120.2 (Fl), 55.6 (Fl), 40.1 (Hex), 35.4 (*t*-Bu), 31.7 (Hex), 31.3 (*t*-Bu), 29.8 (Hex), 24.2 (Hex), 22.9 (Hex), 14.3 (Hex). ^{11}B NMR ($CDCl_3$, δ): 66 ($w_{1/2}$ = 2380 Hz).

Polymerization of B1 and Q1: Synthesis of P1. A solution of **Q1** (15 mg, 0.027 mmol) in 10 mL of CH_2Cl_2 was added to a solution of **B1** (21.1 mg, 0.027 mmol) in 5 mL of CH_2Cl_2, and the mixture was stirred overnight. The volatile materials were removed under high vacuum. The crude material was dissolved in 5 mL of CH_2Cl_2, and the product was precipitated by the addition of 10 mL of hexanes. The polymer was obtained as an orange powdery solid by freeze drying from benzene. Yield: 18.0 mg, 59%. ^{1}H NMR ($CDCl_3$, δ): 8.86 (d, 2H, ^3J = 8 Hz, Q), 8.64 (br, 2H, Q), 7.85 (d, 2H, ^3J = 8 Hz, Q), 7.70 (s, 4H, Ph), 7.66 (d, 2H, ^3J = 6 Hz, Q), 7.58 (d, 2H, ^3J = 8 Hz, Fl), 7.55 (br d, 2H, ^3J = 3 Hz, Fl), 7.44 (br, 2H, Th), 7.39−7.35 (m, 6H, *t*-BuPh and Fl), 7.30 (d, 4H, ^3J = 8 Hz, *t*-BuPh), 7.25 (d, 2H, ^3J = 8 Hz, Q), 7.19 (br, 2H, Th), 1.87 (br, 4H, Hex), 1.30 (s, 18H, *t*-Bu), 1.20−0.95 (br, 12H, Hex), 0.82−0.60 (br, 10H, Hex). ^{13}C NMR ($CDCl_3$, δ): 159.3 (Q), 150.4 (Fl), 149.9, 145.3 (Fl), 144.1, 143.9 (Ph), 140.7 (Fl), 139.8 (Q), 138.1 (Q), 137.8 (Q), 134.1, 133.6 (Fl), 132.3 (Ph), 130.3 (Q), 127.6, 127.0 (Q), 126.4 (Ph), 124.7 (Ph), 124.0, 123.3 (Q), 118.8 (Fl), 118.4, 109.9 (Q), 54.9 (Fl), 40.3 (Hex), 34.6 (*t*-Bu), 31.6 (Hex), 31.6 (*t*-Bu), 29.9 (Hex), 24.2 (Hex), 22.8 (Hex), 14.3 (Hex). ^{11}B NMR ($CDCl_3$, δ): 11 ($w_{1/2}$ = 2100 Hz). GPC-RI: $M_w = 2.07 \times 10^4$, PDI = 1.90. GPC-MALLS (THF, d*n*/d*c* = 0.272 mL/g): $M_w = 1.72 \times 10^4$, PDI = 1.20. UV−vis (CH_2Cl_2, 2.1×10^{-6} M repeat units): λ_{max} = 367, 443 nm. Fluorescence (CH_2Cl_2, 2.1×10^{-6} M repeat units): $\lambda_{em,max}$ = 470, 611 nm (λ_{exc} = 367 nm), Φ = 0.9%. TGA (N_2, 20 °C/min): T_{dec} = 326 °C (onset).

Polymerization of B1 and Q2: Synthesis of P2. A solution of **B1** (107.2 mg, 0.137 mmol) in 10 mL of CH_2Cl_2 was added to a solution of **Q2** (68.5 mg, 0.137 mmol) in 10 mL of CH_2Cl_2 and was stirred overnight. The volatile materials were removed under high vacuum. The crude material was dissolved in 20 mL of CH_2Cl_2, and the polymer was precipitated by the addition of 40 mL of hexanes. A second fraction was obtained by the addition of an additional 20 mL of hexanes. The polymer was isolated by freeze drying from benzene as a yellow powdery solid that was kept under high vacuum for 24 h. Yield: 98 mg, 66%. ^{1}H NMR ($CDCl_3$, δ): 8.55 (d, 2H, ^3J = 8 Hz, Q), 7.85 (d, 4H, ^3J = 8 Hz, Ph), 7.70−7.60 (m, 6H, Q and Ph), 7.60−7.52 (m, 4H, Fl), 7.42−7.28 (m, 12H, Fl and *t*-BuPh and Q), 7.21 (d, 2H, ^3J = 8 Hz, Q), 2.57 (s, 6H, Q-CH_3), 1.85 (br, 4H, Fl-CH_2), 1.33 (s, 18H, *t*-Bu), 1.20−1.00 (br, 12H, Hex), 0.9−0.6 (m, 10H, Hex). ^{13}C NMR ($CDCl_3$, δ): 158.6 (Q), 153.5, 150.1 (Fl), 149.7, 140.8 (Fl), 139.8 (Q), 138.3 (Q), 138.1 (Q), 133.3 (Ph), 132.2, 131.5 (Q), 130.5 (Ph), 129.0, 128.9 (Fl), 127.7 (Ph), 125.6, 125.5, 125.3, 124.7 (Ph), 118.9 (Fl), 109.9 (Q), 54.9 (Fl), 40.6 (Hex), 34.7 (*t*-Bu), 31.9 (Hex), 31.7 (*t*-Bu), 30.1 (Hex), 24.2 (Hex), 22.9 (Hex), 21.4 (Me), 14.4 (Hex).^{11}B NMR (160.3 MHz, δ): 12 ($w_{1/2}$ = 2400 Hz). GPC-RI for fraction 1: $M_w = 2.72 \times 10^4$, PDI = 1.56; for fraction 2: $M_w = 1.26 \times 10^4$, PDI = 1.40. GPC-MALLS for fraction 1: (THF, d*n*/d*c* = 0.207 mL/g) $M_w = 1.66 \times 10^4$, PDI = 1.24; for fraction 2: (THF, d*n*/d*c* = 0.200 mL/g) $M_w = 9.82 \times 10^3$, PDI = 1.30. UV−vis (CH_2Cl_2, 5.3×10^{-6} M repeat units): λ_{max} = 411 nm. Fluorescence (CH_2Cl_2, 5.3×10^{-6} M repeat units): $\lambda_{em,max}$ = 536 nm (λ_{exc} = 314 nm), Φ = 19%. TGA (N_2, 20 °C/min): T_{dec} = 318 °C (onset). Anal. Calcd for $\{C_{77}H_{80}B_2N_2O_2\}_n$: C, 85.07; H, 7.42; N, 2.58. Found: C, 83.93; H, 6.99; N, 2.57.

Conclusions

Boron-induced ether cleavage reactions serve as an exceptionally mild, transition-metal-free method for the preparation of organoboron quinolate polymers with both the boron and quinolato ligands embedded in the polymer main chain. Two polymers with different π-conjugated linkers were prepared. Both of these polymers are readily soluble in common organic solvents and thermally stable to >300 °C. The photoluminescence properties can be tuned by varying the conjugated bridge connecting the quinolato groups. In fact, the degree of conjugation of the linker critically influences the nature of the frontier orbitals, as demonstrated by DFT calculations for molecular model systems. With the highly delocalized Th−C_6H_4−Th linker, the lowest energy absorption corresponds to ICT from this conjugated linker to the pyridyl moiety. In contrast, with a less delocalized biphenyl linker, ICT occurs from the fluorene moiety of the diboron monomer to the pyridyl rings on the basis of time-dependent DFT calculations on molecular model systems. Another interesting phenomenon that is also attributed to the presence of the extended conjugated π system is that the Th−C_6H_4−Th linker leads to a concentration-dependent emission behavior as a result of aggregation phenomena.

Acknowledgment. We acknowledge the National Science Foundation (NSF CHE-0809642) for support of this research. We also thank the NSF for GPC and MALLS instrumentation provided through the NSF-MRI program (MRI 0116066). F.J. is an Alfred P. Sloan research fellow. We thank Prof. Suning Wang and Dr. Yi Cui for kindly providing samples of the ligands Q1 and Q2.

Supporting Information Available: 2D NMR and MALDI-TOF spectra of **P1** and **P2**; details of DFT calculations. This material is available free of charge via the Internet at http://pubs.acs.org.

References and Notes

(1) (a) Tang, C. W.; VanSlyke, S. A. *Appl. Phys. Lett.* **1987**, *51*, 913–915. (b) Tang, C. W.; VanSlyke, S. A.; Chen, C. H. *J. Appl. Phys.* **1989**, *65*, 3610–3616.

(2) Reviews: (a) Chen, C. H.; Shi, J. *Coord. Chem. Rev.* **1998**, *171*, 161–174. (b) Wang, S. *Coord. Chem. Rev.* **2001**, *215*, 79–98. Recent examples: (c) Montes, V. A.; Li, G.; Pohl, R.; Shinar, J.; Anzenbacher, P., Jr. *Adv. Mater.* **2004**, *16*, 2001–2003. (d) Pohl, R.; Montes, V. A.; Shinar, J.; Anzenbacher, P., Jr. *J. Org. Chem.* **2004**, *69*, 1723–1725. (e) Montes, V. A.; Pohl, R.; Shinar, J.; Anzenbacher, P., Jr. *Chem.—Eur. J.* **2006**, *12*, 4523–4535. (f) Zhang, H.; Huo, C.; Ye, K.; Zhang, P.; Tian, W.; Wang, Y. *Inorg. Chem.* **2006**, *45*, 2788–2794. (g) Macedo, F. P.; Gwengo, C.; Lindeman, S. V.; Smith, M. D.; Gardinier, J. R. *Eur. J. Inorg. Chem.* **2008**, 3200–3211. (h) Liddle, B. J.; Silva, R. M.; Morin, T. J.; Macedo, F. P.; Shukla, R.; Lindeman, S. V.; Gardinier, J. R. *J. Org. Chem.* **2007**, *72*, 5637–5646. (i) Son, H. J.; Han, W. S.; Chun, J. Y.; Kang, B. K.; Kwon, S. N.; Ko, J.; Han, S. J.; Lee, C.; Kim, S. J.; Kang, S. O. *Inorg. Chem.* **2008**, *47*, 5666–5676. (j) Zhou, Y.; Xiao, Y.; Li, D.; Fu, M.; Qian, X. *J. Org. Chem.* **2008**, *73*, 1571–1574. Recent examples of fluorescent organoboron chelates for biological applications: (k) Ulrich, G.; Goze, C.; Guardigli, M.; Roda, A.; Ziessel, R. *Angew. Chem., Int. Ed.* **2005**, *44*, 3694–3698. (l) Zhang, G.; Chen, J.; Payne, S. J.; Kooi, S. E.; Demas, J. N.; Fraser, C. L. *J. Am. Chem. Soc.* **2007**, *129*, 8942–8943.

(3) Wu, Q.; Esteghamatian, M.; Hu, N.-X.; Popovic, Z.; Enright, G.; Tao, Y.; D'Iorio, M.; Wang, S. *Chem. Mater.* **2000**, *12*, 79–83.

(4) Cui, Y.; Liu, Q.-D.; Bai, D.-R.; Jia, W.-L.; Tao, Y.; Wang, S. *Inorg. Chem.* **2005**, *44*, 601–609.

(5) Cui, Y.; Wang, S. *J. Org. Chem.* **2006**, *71*, 6485–6496.

(6) Kappaun, S.; Rentenberger, S.; Pogantsch, A.; Zojer, E.; Mereiter, K.; Trimmel, G.; Saf, R.; Möller, K. C.; Stelzer, F.; Slugovc, C. *Chem. Mater.* **2006**, *18*, 3539–3547.

(7) Qin, Y.; Kiburu, I.; Venkatasubbaiah, K.; Shah, S.; Jäkle, F. *Org. Lett.* **2006**, *8*, 5227–5230.

(8) (a) Bao, Z.; Rogers, J. A.; Katz, H. E. *J. Mater. Chem.* **1999**, *9*, 1895–1904. (b) Calvert, P. *Chem. Mater.* **2001**, *13*, 3299–3305.

(9) Wang, X.-Y.; Weck, M. *Macromolecules* **2005**, *38*, 7219–7224.

(10) (a) Qin, Y.; Pagba, C.; Piotrowiak, P.; Jäkle, F. *J. Am. Chem. Soc.* **2004**, *126*, 7015–7018. (b) Qin, Y.; Kiburu, I.; Shah, S.; Jäkle, F. *Macromolecules* **2006**, *39*, 9041–9048.

(11) (a) Nagata, Y.; Chujo, Y. *Macromolecules* **2007**, *40*, 6–8. (b) Nagata, Y.; Chujo, Y. *Macromolecules* **2008**, *41*, 2809–2813. (c) Nagata, Y.; Chujo, Y. *Macromolecules* **2008**, *41*, 3488–3492.

(12) Nagata, Y.; Otaka, H.; Chujo, Y. *Macromolecules* **2008**, *41*, 737–740.

(13) Li, H.; Jäkle, F. *Angew. Chem., Int. Ed.* **2009**, *48*, 2313 −2316.

(14) Extended conjugation through the empty p orbital of tricoordinate boron is well documented: (a) Entwistle, C. D.; Marder, T. B. *Angew. Chem., Int. Ed.* **2002**, *41*, 2927–2931. (b) Entwistle, C. D.; Marder, T. B. *Chem. Mater.* **2004**, *16*, 4574–4585. (c) Jäkle, F. *Coord. Chem. Rev.* **2006**, *250*, 1107–1121. (d) Nagata, Y.; Chujo, Y. In *Boron-Containing Polymers*; Macromolecules Containing Metal and Metal-Like Elements Series; Abd-El-Aziz, A. S., Carraher, C. E., Jr., Pittman, C. U., Jr., Zeldin, M., Eds.; Wiley-Interscience: Hoboken, NJ, 2007; Vol. 8, pp 121−147.

(15) Extrapolation of the relative emission intensity of excimer to monomer (I_{610}/I_{360}) to zero concentration gave a value close to zero, suggesting that excimer formation is primarily due to interchain aggregate formation.

(16) Eaborn, C.; Hornfeld, H. L.; Walton, D. R. M. *J. Organomet. Chem.* **1967**, *10*, 529–530.

(17) *Handbook of Photochemistry*, 2nd ed.; Murov, S. L., Carmichael, I., Hug, G. L., Eds.; Marcel Dekker: New York, 1993.

(18) Frisch, M. J.; Trucks, G. W.; Schlegel, H. B.; Scuseria, G. E.; Robb, M. A.; Cheeseman, J. R. Montgomery, J. A., Jr.; Vreven, T.; Kudin, K. N.; Burant, J. C.; Millam, J. M.; Iyengar, S. S.; Tomasi, J.; Barone, V.; Mennucci, B.; Cossi, M.; Scalmani, G.; Rega, N.; Petersson, G. A.; Nakatsuji, H.; Hada, M.; Ehara, M.; Toyota, K.; Fukuda, R.; Hasegawa, J.; Ishida, M.; Nakajima, T.; Honda, Y.; Kitao, O.; Nakai, H.; Klene, M.; Li, X.; Knox, J. E.; Hratchian, H. P.; Cross, J. B.; Adamo, C.; Jaramillo, J.; Gomperts, R.; Stratmann, R. E.; Yazyev, O.; Austin, A. J.; Cammi, R.; Pomelli, C.; Ochterski, J. W.; Ayala, P. Y.; Morokuma, K.; Voth, G. A.; Salvador, P.; Dannenberg, J. J.; Zakrzewski, V. G.; Dapprich, S.; Daniels, A. D.; Strain, M. C.; Farkas, O.; Malick, D. K.; Rabuck, A. D.; Raghavachari, K.; Foresman, J. B.; Ortiz, J. V.; Cui, Q.; Baboul, A. G.; Clifford, S.; Cioslowski, J.; Stefanov, B. B.; Liu, G.; Liashenko, A.; Piskorz, P.; Komaromi, I.; Martin, R. L.; Fox, D. J.; Keith, T.; Al-Laham, M. A.; Peng, C. Y.; Nanayakkara, A.; Challacombe, M.; Gill, P. M. W.; Johnson, B.; Chen, W.; Wong, M. W.; Gonzalez, C.; Pople, J. A. *Gaussian 03*, revision C.02; Gaussian, Inc.: Wallingford, CT, 2004.

MA9001319